RF PHOTONICS

INTRODUCTION & EXECUTIVE SUMMARY

Photonics and Radiofrequency (RF) are two key communication technologies, usually associated to wired and wireless transmission media respectively due to the low transmission losses at their respective frequency range. Optical wired links, based on optical fibers, exhibit transmission losses as low as 0.2 dB/km at 1500 nm wavelength (193 THz). On the other hand, RF wireless links, operating mainly in the microwave frequency range (3 GHz – 30 GHz) experience atmospheric attenuation below 0.1 dB/km. Both technologies are the cornerstone of current mobile communication networks that allow users to move freely within the area of coverage.

Over the past years, we have observed the exponential increase of mobile communications data rates, demanded by an increasing number of mobile services. The trend, established in 2004 and known as Edholm's law of bandwidth, predicts that the bandwidth and data rates double every 18 months. To address this trend, wireless carriers started to show interest in upper regions of the electromagnetic spectrum where there is available bandwidth, which include the millimeter-wave (MMW, 30 GHz – 300 GHz) and the Terahertz (THz, 300 GHz – 3 THz) bands. Over the past 5 years E-band (60 GHz – 90 GHz) has increased 500%, reaching 6% of the total installed microwave base, becoming a key technology for 5G deployment. The current vision for the 6G considers the access to the upper end of the MMW range necessary to push the boundaries of connectivity, providing minimum latency and reliable connectivity to enable innovations as autonomous driving, seamless extended reality, and the integration of artificial intelligence (AI) on a massive scale.

However, using the frequency bands above 100 GHz is still today a challenge. This requires closing what has traditionally been known as the "Terahertz gap", which has been elusive for many decades now due the difficulties in realizing powerful sources and efficient receivers. These issues will be sorted out most likely through the hybrid integration of photonics, electronics, and RF engineering technologies as is happening in the pluggable scenario. In this line, key issues will appear such as the lack of high-frequency interconnection technologies as well as the lack of measurement routines and test and measurement instruments above 220 GHz.

RF PHOTONICS PURPLE BRICK WALL

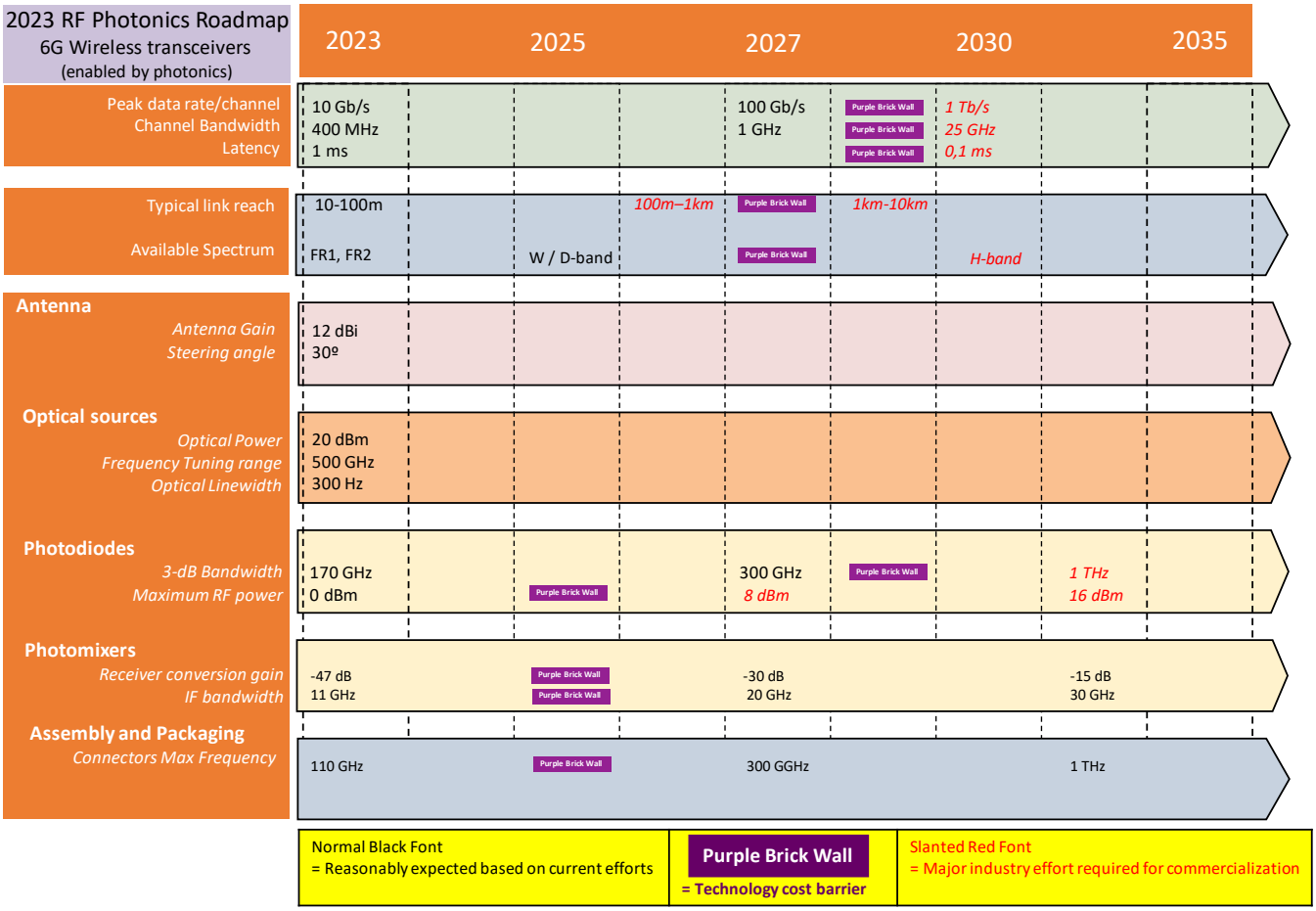

One of the main drivers of RF Photonics modules are mobile communications, which evolve through successive generations approximately every 10 years. As shown in **Table 1**, since the fourth generation (4G), which in 2009 started to provide broadband connectivity that reached up to 1 Gbps by LTE-Advanced (LTE, Long Term Evolution) technology, every new generation has continued to improve the Key Performance Indicators (KPI). Since the world's first 6G White Paper was published in September 2019 by the finish 6G Flagship[1], academia and industry initiated the definition of what eventually will be the next generation (6G), with efforts launch at different countries[1]. For the radio technology and signal processing, the requirements for 6G are reaching Tb/s data throughput and sub-ms latency to the networking layer, in addition to extremely high reliability with packet error rate as low as 10^{-8} and extreme energy efficiency/ultra-low energy consumption, together with very high security and cm-level accuracy localization [3]. In addition, these advances need to be achieved jointly utilizing licensed and unlicensed spectrum, re-farming and efficiently reusing current 5G and other legacy systems. This exponential increase in capacity requires a massively increase in the amount of available spectrum, located at the higher regions of the electromagnetic spectrum in the millimeter-wave (MMW, 30 GHz – 300 GHz) and the Terahertz (THz, 300 GHz – 3 THz) bands.

This need has already been addressed by the US Government in 2019 when the FCC opened the 95 GHz to 3 THz frequency range for experimental use and by reserving selected bands for unlicensed applications. Considering the challenges imposed by the law of physics, this frequency range is still known as the "Terahertz gap" , which has been elusive for many decades now due the difficulties in realizing powerful sources and efficient receivers. It is expected that commercially available THz communication systems will require a joint effort in waveform and modulation, radio channel characterization, beamforming and feasibility of hardware together. The radio building blocks need to be further developed to meet stringent 6G requirements.

Other industry drivers for THz systems are imaging and spectroscopy, where the maturity of the available technology has reached the level of enabling real-world use.

Table 1 *Key Performance Indicator evolution with successive generations of wireless standards*

Key Performance Indicator (KPI)	4G	5GNR	6G
Year	2009	2018	2030
Frequency Band (GHz)	0.6 to 5.925	3,5 (FR1) 28 (FR2)	100 – 300 (Sub-THz bands)
Channel Bandwidth (MHz)	20	100 (FR1) 400 (FR2)	1000
User Equipment Transmitter Power (dBm)	+23	+26	
Peak data rate (Gbps)	1	20	1000
Capacity (Tbps/km2)	-	15	150
User latency (ms)	60	1	0.1
Energy efficiency		1x	10x
Reliability		99.9999%	99.99999%

RF Photonics building blocks and key parameters:

RF photonics (RFP) employs photonic technologies to generate, process, control and distribute signals with frequencies above 100 GHz. There are two main RFP modules. On one hand, RFP transmitters, which use photonic technology to generate RF carrier frequencies. On the other, RFP receivers, using photonic techniques to down-converting the modulated RF carrier received to an Intermediate-Frequency (IF) or to a baseband (BB) electronic signal.

The building blocks of an RFP transmitter system is shown in ***Figure 1***, include:

- **Optical signal generator**, usually based on infrared lasers emitting at 1550 nm, producing continuous-wave single wavelength laser light or short optical pulses at a defined repetition rate. This is a crucial difference establishing two types of MWP systems, frequency-domain or time-domain.
- **Optical modulator**, which performs the Electrical-to-Optical (E/O) conversion used to bring the high-speed data signals into the optical domain. RF bandwidths of 20 GHz are typical of optical modulators on InP, reaching up to 500 GHz in plasmonic devices.
- **Optical amplification**, used to compensate for the insertion losses (signal propagation losses) of the optical functional building blocks, which can be placed at any point in the optical path
- **Optical signal processing unit**, which can perform an added functionality (RF up/down conversion, optical filtering, optical delay, optical beam forming …) in the optical domain, and
- **Optical-to-Electrical (O/E) converter**, to generate the RF signals in the electrical domain, followed by an electrical RF amplifier and an antenna element to radiate the RF.

The most critical parameters that need to be address for MWP transmitters pertain to the optical signal generator, for which increasing the generated optical power and the reduction of amplitude and phase noise are key parameters. Other key element, responsible for the emitted RF power, are the O/E converters. The performance of the system is ultimately limited by these critical parameters.

An RFP receiver has two main possible configurations, shown in ***Figure 2***, are:

- **Optoelectronic down-conversion**: Mixing the received RF with a Photonic Local Oscillator (PLO) in a high-speed photomixer. Tuning the frequency of the PLO, the receiver can cover a wide range of carrier frequencies. The most common photomixer is a Photo-Conductive Antenna (PCA) [4], although photodiodes have also been explored for down-conversion [5][6]. Photoconductive devices are fabricated on Low Temperature GaAs (LT-GaAs), and more recently on InP and iron (Fe) doped InGaAs, not all of which are easily integrated. Novel types of O/E converters, such as the plasmonic internal-photoemission detectors (PIPEDs)[7], are currently being developed to enable RF Photonic transmitter and receiver integration on a silicon photonic platform.
- **Optical modulator-based receiver**: The other configuration of a RF photonic receiver, also shown in Figure 2, has blocks that are like those in a RF photonic transmitter.

The most critical parameter that need to be address for MWP receivers are decreasing the receiver conversion loss and increasing the sensitivity.

At system level, the key figures of merit for the MWP systems are link gain, noise figure and phase noise, input/output intercept points, spurious free dynamic range (SFDR), and output power. These metrics show the impact of losses, noise, and nonlinearities [8]. The relative importance of these metrics and the specific values that are desired for the metrics depend on the application. For example, a Radio-over Fiber (RoF) link that carries digital or PAM-4 signals modulated on a RF carrier would have a different requirement for the SFDR than a radar link. A link for generation of a millimeter-wave signal for transmission from an antenna may have a strong requirement on the saturation power but not necessarily on the SFDR.

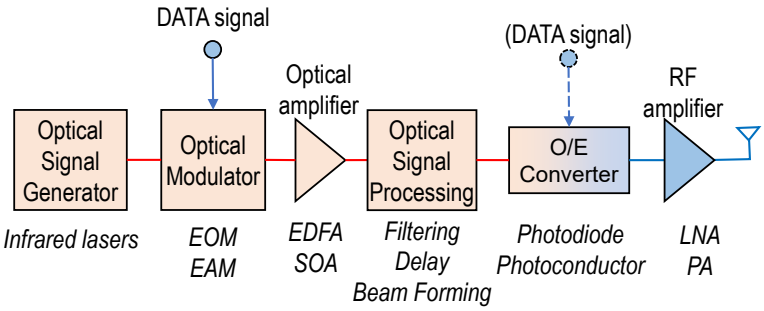

Figure 1 *Schematic of the building blocks of a MWP transmitter. EOM: electro-optic modulator, EAM: electro-absorption modulator, EDFA: Erbium-doped fiber amplifier, SOA: semiconductor optical amplifier, LNA: low-noise amplifier, PA: power amplifier.*

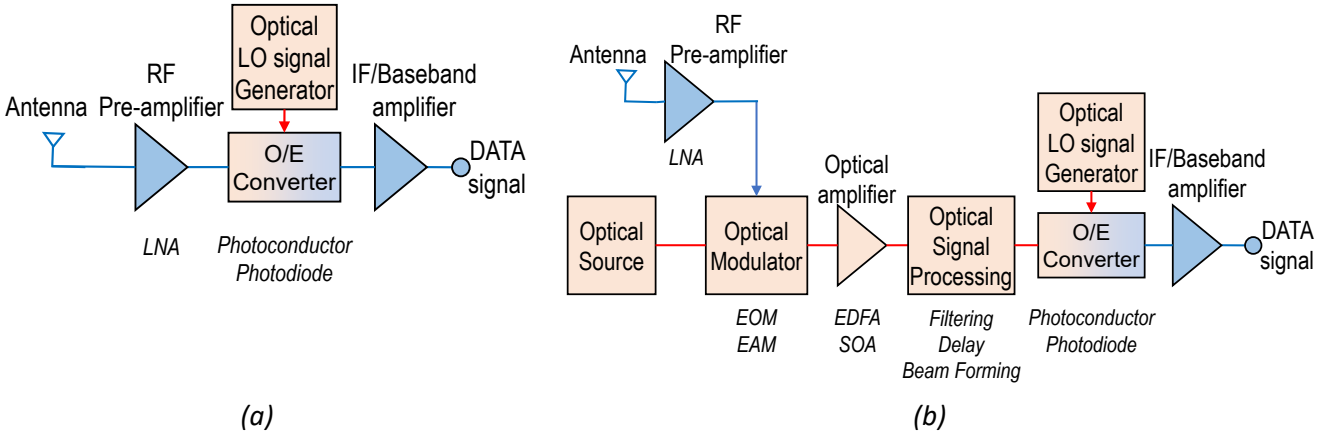

Figure 2 *Schematic of the building blocks of a RF Photonic receiver based on: (a) Photomixer detector, and (b) RF-to-Optical direct detection. LNA: low-noise amplifier, IF: intermediate frequency, EOM: electro-optic modulator, EAM: electro-absorption modulator, EDFA: Erbium-doped fiber amplifier, SOA: semiconductor optical amplifier.*

Terahertz Optical Signal Generator sources

There are two main types of photonic THz systems depending on the employed photonic source, categorized into time domain or frequency domain. Time domain systems are based on optical down-conversion, shining femtosecond pulsed lasers into photoconductive antennas (PCA) to down-convert light frequencies down to the THz range. Frequency domain systems employ continuous-wave (CW) laser beams that are down-converted into THz signals through optical heterodyning. Optical heterodyning is the technique that presents key advantages over the rest, including all-electronics approaches, among them (i) the bandwidth, (ii) the maximum RF frequency and (iii) the frequency tuning range.

Optical heterodyne employs two optical wavelengths λ_1 and λ_2 that are mixed onto a high-speed photo-mixer (photodiode or photoconductor), generating an electrical signal at the difference frequency between the optical wavelengths, $f_{beat} = c|\lambda 1 - \lambda 2|/(\lambda 1\, \lambda 2)$. There are different approaches to generate the two optical wavelengths, being the most straightforward method to combine the optical output of two different single-frequency lasers as shown in ***Figure 3(a)***. While its main advantages are its maximum achievable RF frequency (up to 2.5 THz) and the broad tuning range (from 5 GHz to 2.5 THz), the frequency stability is generally poor if the two lasers are free running, with wide linewidth and large frequency drift (> 10 MHz/h). This required using additional phase locking schemes [9] to increase the signal stability.

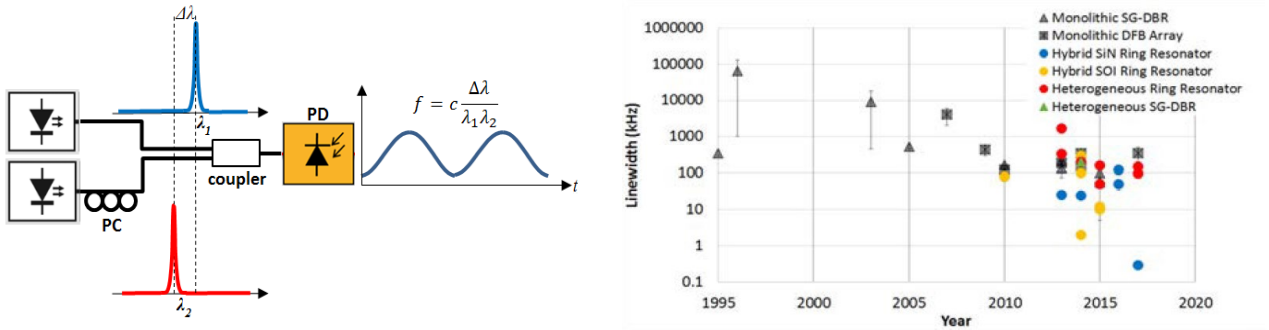

(a) (b)

Figure 3 *Photonic optical heterodyne signal generation system: (a) key building blocks, including two single-wavelength lasers, at least one being wavelength tunable, an optical combiner (coupler) and a photodiode (PD), (b) Linewidth of widely tunable integrated lasers versus time. Monolithic is III–V-integration, hybrid is individual III–V dies bonded, soldered or butt-coupled to another substrate material, and heterogeneous larger pieces of the III–V gain material are bonded to silicon. SG–DBR: Sampled grating distributed Bragg reflector, DFB: distributed feedback, SiN: silicon-nitride, SOI: silicon-on-insulator. (from [16])*

Photonic integration has been a key technology for improving the stability of optical heterodyne sources through [10]: a) sharing the same Peltier cooler and experiencing the same environmental fluctuations, and b) distances become shorter, to improve the efficiency of delay sensitive electronic Optical Phase-Locked-Loop (OPLL) [11]. Indium-Phosphide (InP) monolithic integration of two DFB lasers has been demonstrated, as shown in ***Figure 3(b)****, thereby reducing the linewidth below 300 kHz for cavity lengths of 2500-µm and achieving RF beat note linewidths below 1-MHz for frequencies ranging from 2.5 GHz to 20 GHz [10]. With this approach, a fully integrated millimeter-wave transmitter on InP was demonstrated [12]. The wavelength tuning range of each DBF laser was about 1.5 nm (~ 188* GHz) and the optical linewidth was greater than 1 MHz. The advantage of the integrated approach was demonstrated when the frequency tuning range was extended above 2 THz by integrating a four DFB laser array combining standard optical element building blocks (BB) from an InP photonic integration foundry platform [13]. Currently, hybrid integration technology has also been considered for integrating optical heterodyne generators. A photonic microwave generator on a heterogeneous silicon-InP platform was demonstrated, with lasers that tune over 42 nm and having less than 150 kHz linewidth, generating RF signals from 1 to 112 GHz [14]. Terahertz signal generation at 330 GHz was demonstrated using an InP/Polymer hybrid integrated optical heterodyne source, including two Distributed Bragg Reflector (DBR) lasers and a Y-junction optical combiner [15]. As shown in ***Figure 3(b)***, hybrid and heterogeneous integration technologies contribute to the reduction the optical linewidth. Linewidths of individual lasers down to few hundred Hertz have been demonstrated.

To improve the stability of the optical heterodyne technique, there are several alternatives. One is to use optical injection locking, injecting into each of the two lasers the output of an Optical Frequency Comb (OFC), an optical source that produces many phase locked optical wavelengths with a fixed frequency spacing between them. It has been shown that 2.8 MHz optical linewidth lasers could generate a 330 GHz beat note signal with 12 kHz linewidth when injection locked. A growing number of OFCG implementations are becoming available. The most common is to use a single-mode laser followed by optical amplitude and/or phase modulators, generating multiple optical sidebands around the optical carrier frequency spaced by the RF Continuous-Wave (CW) source frequency driving the modulator. However, phase noise performance of such a solution depends on the multiplication factor M, with respect to the fundamental driving RF frequency, i.e., the obtained phase noise

power spectral density is equal to M^2 times the phase noise of the employed driving RF signal, like any nonlinear electronic frequency multiplier. Currently, a new range of OFCG produced by non-linear optical methods such as the Kerr combs resulting from four wave mixing in micro-ring resonators. Micro-integration technology has been used to generate a comb of frequencies across 50 nm of the optical spectrum which allows locking of a semiconductor laser to any comb line. Thus, the optical comb can be used as a reference for locking several tunable semiconductor lasers.

Another route to improve the stability of optical heterodyning is to generate the two wavelengths from a single Continuous-Wave (CW) laser through external modulation in a Mach-Zehnder Modulator (MZM) driven by an RF CW source [17]. With this approach, the generated RF signal is a multiple of the RF CW source frequency from which it inherits the phase noise. Different schemes have been proposed to increase the generating two optical wavelengths at twice the RF synthesizer frequency, thereby doubling the frequency of the CW synthesizer. Higher multiplication factors can be achieved by taking advantage of the inherent nonlinearity of the optical modulator response to generate high-order optical sidebands. Quadrupling of the CW synthesizer has been reported, however, to date all these demonstrations have been based on commercially available discrete components.

Optoelectronic converters (photomixers)

Photodiodes

Photodiodes are key components used to translate signals from the optical domain to the RF domain. Photodiodes operate as a square law detector, rectifying the optical frequencies. When two optical frequencies are input, it generates a photocurrent which has a frequency equal to the difference frequency between the optical frequencies.

The most widely optoelectronic converter is the p-i-n photodiode (PIN-PD), which is formed by an intrinsic absorption layer sandwiched between positively (p-type) and negatively (n-type) doped semiconductor layers. The most common PIN-PDs suitable for monolithic integration are based either in Ge-on-Si or in InP and lattice-matched III-V semiconductors (such as InGaAs). As shown in **Table 2**, both platforms can produce PIN-PD with good responsivity (~ 1 A/W), low dark currents (few nA), and relatively large bandwidth (> 30 GHz). State-of the-art, monolithically integrated Ge-on-Si and InP PIN-PDs can achieve bandwidths over 80 GHz [19][20]. In PIN-PDs however there is a strong trade-off between bandwidth and maximum RF power, another key requirement.

Table 2 *comparison of photodetectors*

Type	UTC-PD	PIN-PD	PIN-PD	UTC-PD
Year	2010	2011	2014	2023
Integration platform	InGaAs/InP	Ge-on-Si	InGaAs/InP	InGaAs/InP
Bandwidth (GHz)	170	120	80	280
Responsivity (A/W)	0.27	0.8	0.55	0.25
Dark current (nA)	-	4×10^3 (-1 V)	5 (3 V)	10 (4 V)
Output power (dBm)	-9 (200 GHz)	-	-	- 0.6 (240 GHz)
Output coupling	GSG			WR3.4
Reference	[24]	[19]	[20]	[22]

To exceed the limitations associated with PIN-PDs, the uni-travelling carrier photodiode (UTC-PD) was proposed, where only electrons contribute to the photocurrent to reduce the transient time and allow for higher bandwidth. Furthermore, UTC-PDs exhibit reduced space-charge effects and, as a result, saturation occurs at higher levels of photocurrent relative to PIN-PDs. The maximum reported output power from UTC-PD is around 537 mW at 240 GHz, and about 100 nW at 0.7 THz [21][22]. An additional increase of the output power by a factor of two or three can be obtained through impedance matching circuits that reduce the RC-limit [23].

While most state-of-the-art photonic THz emitters employ waveguide-coupled photodiodes as active elements, the monolithic integration of all the building blocks in a transmitter system shown in ***Figure 1*** remains a challenge. The epi-layer structure of an InP-based UTC-PD is different from the structure of a laser or EA modulator, thus it is challenging to integrate the UTC-PD with other active components based on InP. Two such demonstrations have been reported, one an InP monolithic integration including a UTC-PD with 3-dB bandwidth of 170 GHz [24][12] and a second one by heterogeneously integration silicon-InP with a high speed photodiodes with 3-dB bandwidth of 65 GHz [25].

Photoconductors

While photodiodes are the choice for photonic THz emitters, photonic THz receivers are based on vertically illuminated Photoconductive Antennas (PCAs), which can operate as either an emitter or a receiver of THz radiation. PCA consists of two metallic electrodes, patterned on the surface of a highly resistive semiconductor material, defining a microscale gap between them. When the THz radiation signal is received by the antenna, a THz electric field is induced in the gap, which accelerates the photocarriers created at the gap by an optical pump beam. For CW THz detection, the optical pump beam comes from a pair of lasers with a frequency difference close to the received THz radiation. When modulated, this allows the direct down-conversion of the data signals from the W-, D-, and THz-band to the baseband or an intermediate frequency (IF) signal using a photonic Local Oscillator.

Since PCAs do not generate a noteworthy current in the absence of a THz signal are therefore electrical shot noise free. In addition, the fact that the semiconductor is highly resistive, even under illumination, results in a small thermal noise current. It is only the laser noise that may affect the overall system noise [26]. CW PCA receivers have reached down to noise equivalent power of NEP = 1.8 fW/Hz at 188 GHz [93]. This leads to systems with dynamic ranges (DNRs) up to 117 dB with 4 THz bandwidth.

To date, very few wireless data transmission demonstrations have used photonic THz receivers, as these typically exhibit low conversion gain (defined by the ratio of the IF signal power at the PCA output and the THz power incident on the device) and low IF bandwidth. A recent demonstration has reported a PCA receiver achieving error-free transmission of 4-QAM signals for data rates up to 12 Gbit/s at carrier frequencies up to 320 GHz over a link distance of 1 m. In this demonstration the PCA had an IF bandwidth of 11 GHz and a conversion gain of -47 dB. For comparison, electronic mixer-based receivers exhibit IF bandwidths and conversion gains of up to 32 GHz and −15 dB respectively. The link performance, mainly determined by the received SNR, can be improved either by increasing the emitter power or using array configurations to increase the effective antenna gain.

Planar antennas

To fully exploit the broadband capabilities of photodiodes and photoconductors, it is common to integrate them with planar antennas (such as bow-tie, patch, or slot antennas). This allows to reach higher frequencies, without the restrictions of the coplanar waveguides (CPWs) and related RF-probes.

Planar antennas are widely used for THz photomixers due to the advantage of enabling monolithic integration with the component avoiding the need to make electrical interconnects between the antenna and the photomixer contact pads, critical above 100 GHz. Ultrawideband antennas take advantage of the wide operating frequency range of photomixers. Due to the high permittivity of semiconductors (ε_{SC} = 9.6) and electrically large thickness of the substrates typically used (for 1550 nm InP photomixers, 350 µm >> λ_{THz}), most of the generated power is dissipated in the substrate because of total internal reflections (TIR). Using planar antennas requires to add a hyper- or semi-spherical lenses, attached to the backside of the substrate to to allow interfacing the semiconductor with the air as well as collimate the radiated beam. The higher the lens diameter, the higher the antenna gain that can be achieved (up to 25 dBi for a 20 mm diameter lens).

Antenna Arrays

To increase the emitted power from transmitters, spatial power combination of multiple elements can be used. This method has the advantage of summing the power of each element providing antenna gain. It is worth highlighting that the photonic-approach to antenna arrays has a key advantage, which is enabling the optical distribution of the signal to each of the individual elements of the array through low-loss optical waveguides. Due to the high gain required at these frequency bands, antenna arrays with large number of elements are required. In the case of electronic-driven arrays, we face the serious problems associated with the ohmic losses of the feeding network. As shown in **Figure 4**, for an array of patches, the gain cannot be increased beyond a maximum by increasing the size of the array. The maximum gain depends on the feeding network losses (represented by the attenuation α -expressed in dB/λ-).

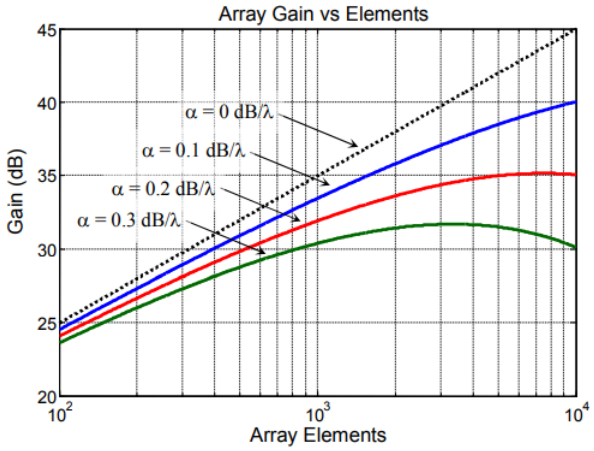

Figure 4: *Array Gain versus Number of elements for different values of loss associated to the feeding network [27]*

To estimate the number of antennas required in the array, one can use as reference the first 10 km Fixed Wireless Access (FWA) demonstration operating at 120 GHz, with 16 dBm output power and 52 dBi gain Cassegrain antennas in transmitter and receiver [28]. The major source of link loss is due to Free Space Path Loss (FSPL), determined by the relation [29]:

$$L_{FSPL} = 92.4 + G_{TX} + G_{RX} + 20 \log f(\text{GHz}) + 20 \log d(\text{km}) + A \cdot d \ \text{dB} \quad (1)$$

where G_{TX} and G_{RX} are the gain in dB of the transmit and receive antennas, f is the frequency in GHz, d is the distance in km and A is the atmospheric absorption in dB/km. Based on this relationship, the required G_{TX} and G_{RX} for covering 10 km link distance at 240 GHz requires 50 dBi antennas.

Unfortunately, dielectric lenses cannot be used for antenna array structures. As the dielectric lens is electrically large compared to the carrier wavelength, the required distance between antenna elements in the array cannot be accomplished, leading to the creation of grating lobes. Therefore, an alternative to silicon lenses is required.

Recently, two approaches have been reported implementing 1x4 photodiode linear antenna transmitter arrays. The first is based on PIN photodiodes with bow-tie antennas that use a cylindrical lens [30] and the second is based on UTC photodiodes with planar-slot-antennas [31]. Both achieved similar results increasing the output power by 10 dB respect to the single antenna element and 20º steering angle. A novel approach is based on Dielectric Rod Waveguide Antennas (DRWA), which are single antenna lensing structures that do not block the development of an array. DRWA are dielectric waveguides which allow to properly radiate the power to the air by tapering their termination [33]. The advantages of this approach are:

- Small form factor dielectric waveguides (smaller than 1 mm x 0,5 mm) allow each antenna element on the chip to have its own DRWA while maintaining the spacing of the array. This contrasts with dielectric lenses, commonly used by the THz industry, with diameters of several millimeters (> 5 mm), blocking arrays.
- The length of the tapered termination is directly related to the antenna directivity. A length of 15 mm leads to gains of around 16 dBm, which is 10 dB below the common gain of dielectric lenses.
- Low gain allowing for radiating angles of about 120 º, required to enable beam steering. This contrasts with dielectric lenses, which have gains up to 25 dB, blocking steering.

A demonstration of the concept was demonstrated with a 16 element DRWA array in a 4x4 configuration feed from rectangular waveguides. The structure showed a total gain of 23.5 dB [32]. From the current gain of a single element DRWA, around 16 dBi, and using the scaling of the antenna array gain with the number of elements, it is estimated (see **Table 3**) that the DRWA array would need between 1000 to 10000 elements.

In addition to the large number of elements in the array, it is worth taking into account that the spacing between the antenna elements of the array reduces as the frequency increases. As shown in **Table 4**, the optimum spacing which would avoid grating lobes reduces from 400 µm at 100 GHz to just 70 µm at 500 GHz. The main problem of large arrays turns now into an assembly and packaging issue.

Table 3 *Gain versus number of Dielectric Rod Waveguide Antenna elements in the array*

DRWA Gain (dBi)	Number of elements	Array Gain Scaling (dB)	Total Gain (dBi)
16	4	6	22
16	16	12	28
16	36	15	31
16	100	20	36
16	1000	30	46
16	10000	40	56

Table 4 *Decreasing size of the antennas with frequency for individual antenna elements.*

Frequency f (GHz)	Wavelength in Air λ (mm)	Wavelength in InP λ (mm)	Antenna Spacing λ /2 (mm)
100	3.0	0.83	0.415
200	1.5	0.42	0.21
300	1.0	0.28	0.14
500	0.5	0.14	0.07

Test, assembly and packaging

Assembly and packaging processes are fundamentally oriented towards providing a physical housing for the integrated circuits, together with reliable signal interconnections between the devices and the world outside the package. However, as the operating frequency increases, several challenges associated with signal loss, dimensions, and fabrication become more critical [34].

Lack of reliable and broadband RF probes for Wafer Level Testing (WLT)

Radiofrequency (RF) test probes are needed for on-wafer measurements characterizing the 6G components during their development. Above 100 GHz, the contact between the current test probes and the semiconductor wafer greatly influences the measurements, in the worst case turning them unreliable. A non-contact head providing more reliable and repeatable probing in the millimetre wave (MMW, 30 GHz to 300 GHz) and Terahertz (THz, 300 GHz to 3 THz) ranges has been long sought.

Moreover, RF test probes are connected to test equipment through RF connectors, which usually limit the operating frequency range of the probe [35]. Standardized coaxial connectors are commonly used, providing a continuous operating frequency range from DC (0 Hz) up to a maximum frequency determined by the type of coaxial connector: 40 GHz for the 2.92 mm (K) connector, 67 GHz for the 1.85 mm connector and more recently, 110 GHz with the 1 mm connector and 220 GHz for the 0.6 mm [36]. For frequencies above 220 GHz, the dimensions of coaxial become impractically small and rectangular waveguide interconnects become the only option. These allow interconnects up to 1.1 THz, with the important drawback as shown in **Figure 5** of being band limited.

Currently there are no probes that continuously cover the frequency range of 6G devices.

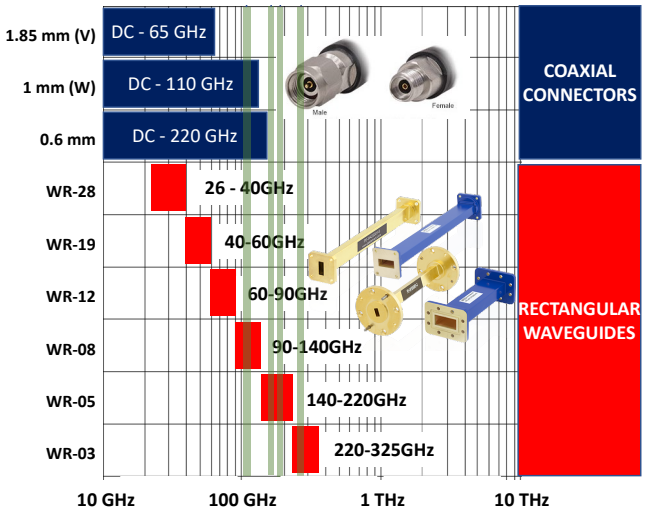

Figure 5: *Frequency range of different coaxial and rectangular waveguide connector standards.*

Lack of high-frequency circuit interconnection technologies

6G components require reliable signal interconnections in their packages. The electronics industry mainly uses wire bond (gold wires) technology which limits the operating frequency well below 220 GHz. To minimize its effects, the wire length should be kept as short as possible, requiring in occasions be shorter than the fabrication tolerance [35]. In addition, gold wires are a different interconnection technology from RF test probes used in component testing, therefore introducing new and unforeseen effects at device packaging.

Lack of measurement routines and systems above 220 GHz

Current broadband Vector Network Analyzer (VNA) systems to measure S-parameters over frequency are limited to 220 GHz. Broadband systems are configured to include banded modules that require engineers to change modules along with complicated calibration and analysis of the data. Needs for on-wafer measurements of 6G components span the range of 70 kHz to 300 GHz in a single sweep. Further, new measurement routines need to be developed to reach highest sensitivities.

Coordinator
Guillermo **Carpintero**, Professor, Department of Electronics Technology, Universidad Carlos III de Madrid, Spain

References:

[1] http://jultika.oulu.fi/Record/isbn978-952-62-2354-4

[2] "Mobile Communications Towards 2030" A 5G Americas White Paper, November 2022.

[3] The 5G Infrastructure Association, "European Vision for the 6G Network Ecosystem" June 2021

[4] T. Harter, S. Ummethala, M. Blaicher, , et al., "Wireless THz link with optoelectronic transmitter and receiver," Optica 6, 1063-1070 (2019)

[5] T. Nagatsuma, A. Kaino, S. Hisatake et al. "Continuous-wave Terahertz Spectroscopy System Based on Photodiodes," PIERS Online, vol. 6, no. 4, pp. 390-394, 2010.

[6] E. Rouvalis, M. J. Fice, C.C. Renaud, A.J. Seeds, "Millimeter-wave optoelectronic mixers based on uni-traveling carrier Photodiodes," IEEE Trans. Microwave Theory and Techniques, Vol. 60, pp. 686-691, 2012.

[7] T. Harter, S. Muehlbrandt, S. Ummethala, et al. "Silicon–plasmonic integrated circuits for terahertz signal generation and coherent detection," Nature Photon 12, 625–633 (2018).

[8] D. Marpaung, J.Yao & J. Capmany, "Integrated microwave photonics". Nature Photon 13, 80–90 (2019)

[9] K. Balakier, L. Ponnampalam, M. J. Fice, C. C. Renaud and A. J. Seeds, "Integrated Semiconductor Laser Optical Phase Lock Loops," in IEEE Journal of Selected Topics in Quantum Electronics, vol. 24, no. 1, (2018)

[10] F. van Dijk, A. Accard, et al. "Monolithic dual wavelength DFB lasers for narrow linewidth heterodyne beat-note generation," Int. Top. Meet. on Microwave Photonics, Singapore, pp. 73-76 (2011)

[11] R.T. Ramos, A.J. Seeds "Delay, linewidth and bandwidth limitations in optical phase-locked loop design" Electronics Letters Volume: 26 , Issue: 6 (1990).

[12] F. van Dijk et al., "Integrated InP heterodyne millimeterwave transmitter," IEEE Photon. Technol. Lett., vol. 26, no. 10, pp. 965–968, (2014).

[13] M. Sun et al., "Integrated four-wavelength DFB diode laser array for continuous-wave THZ generation," IEEE Photon. J., vol. 8, no. 4, pp. 1–8, (2016).

[14] J. Hulme et al., "Fully integrated microwave frequency synthesizer on heterogeneous silicon-iii/v," Opt. Express, vol. 25, no. 3, pp. 2422–2431, (2017).

[15] G. Carpintero et al. "Wireless Data Transmission at Terahertz Carrier Waves Generated from a Hybrid InP-Polymer Dual Tunable DBR Laser Photonic Integrated Circuit" Nature Scientific Reports Vol. 8, (2018)

[16] T. Komljenovic, D. Huang, P. Pintus, M. A. Tran, et al. "Photonic Integrated Circuits Using Heterogeneous Integration on Silicon," in Procc. IEEE, vol. 106, no. 12, pp. 2246-2257, Dec. 2018.

[17] G. Qi et al. "Generation and distribution of a wide-band continuously tunable Millimeter-Wave signal with an Optical External Modulation Technique," IEEE Trans. Mic. Theo. Tech., 53(10), pp. 3090-3097 (2005).

[18] Liu, J., Lucas, E., Raja, A.S. et al. Photonic microwave generation in the X- and K-band using integrated soliton microcombs. Nat. Photonics 14, 486–491 (2020).

[19] Laurent Vivien et al., "Zero-bias 40Gbit/s germanium waveguide photodetector on silicon," Optics Express, vol. 19, no. 11, p. 1096, 2011.

[20] P. Runge et al., "80GHz balanced photodetector chip for next generation optical networks," 2014, doi: 10.1364/ofc.2014.m2g.3.

[21] J. P. Seddon, M. Natrella, X. Lin, C. Graham, C. C. Renaud, and A.J. Seeds, "Photodiodes for terahertz applications," IEEE J. Sel. Topics Quantum Electron., vol. 28, no. 2, Mar./Apr. 2022, Art. no. 3801612.

[22] M. Grzeslo et al., "High saturation photocurrent THz waveguide-type MUTC-photodiodes reaching mW output power within the WR3.4 band," Opt. Exp., vol. 31, no. 4, pp. 6484–6498, 2023.

[23]J.-M. Wun, H.-Y. Liu, Y.-L. Zeng, et al “High-power THz-wave generation by using ultra-fast (315 GHz) uni-traveling carrier photodiode with novel collector design and photonic femtosecond pulse generator,” in Proc. Opt. Fiber Commun. Conf., 2015, Paper M3C. 6
[24]E. Rouvalis et al., “170 GHz uni-traveling carrier photodiodes for InP-based photonic integrated circuits,” OPTICS EXPRESS 20090, vol. 58, no. 11, pp. 1716–1718, 2010.
[25]J. Hulme et al. "Fully integrated microwave frequency synthesizer on heterogeneous silicon-III/V," Opt. Express 25, 2422-2431 (2017)
[26]S. Makhlouf *et al*., "Terahertz Sources and Receivers: From the Past to the Future," in *IEEE Journal of Microwaves*, vol. 3, no. 3, pp. 894-912, July 2023
[27]R.V. Gatti et al “Flat-profile active scanning antenna for satellite terminals in Ku-band operating on new fast trains generation” 28th ESA Antenna Workshop on Satellite Antenna Technology ESTEC, Noordwijk, The Netherlands (May 2005)
[28]A. Hirata et al., "120-GHz-Band Wireless Link Technologies for Outdoor 10-Gbit/s Data Transmission," in IEEE Transactions on Microwave Theory and Techniques, vol. 60, no. 3, pp. 881-895, March 2012.
[29]G. Ducournau, T. Nagatsuma “Wireless Communications in the THz range” in Fundamentals of Terahertz Devices and Applications. Ed. D. Pavlidis John Wiley (2021).
[30]S Nellen et al. "Photonic-enabled beam steering at 300 GHz using a photodiode-based antenna array and a polymer-based optical phased array," Opt. Express 30, 44701-44716 (2022)
[31]M. Che, K. Kondo, H. Kanaya and K. Kato, "Arrayed Photomixers for THz Beam-Combining and Beam-Steering," in *Journal of Lightwave Technology*, vol. 40, no. 20, pp. 6657-6665 (2022)
[32]A. Rivera-Lavado, L.E. García-Muñoz, A. Generalov et al. “Design of a Dielectric Rod Waveguide Antenna Array for Millimeter Waves”. J Infrared Milli Terahz Waves 38, 33–46 (2017).
[33]S. Kobayashi, R. Mittra and R. Lampe, "Dielectric tapered rod antennas for millimeter-wave applications," in IEEE Transactions on Antennas and Propagation, vol. 30, no. 1, pp. 54-58, January 1982
[34]Song, H.J. “Packages for Terahertz Electronics,” in Proceedings of the IEEE, vol. 105, no. 6, pp. 1121-1138 (2017)
[35]A. Rumiantsev and R. Doerner, ”RF Probe Technology: History and Selected Topics,” IEEE Microwave Magazine, vol. 14, no. 7, pp. 46-58, Nov.-Dec. 2013
[36]Anritsu “New VNA Technologies Enable Millimeter-Wave Broadband Testing to 220 GHz” [White Paper] (2020)